Solid-state NMR sequential assignment of an Amyloid-β(1–42) fibril polymorph

Author(s):
Ravotti, Francesco; Wälti, Marielle A.; Güntert, Peter; Riek, Roland; Böckmann, Anja; Meier, Beat H.

Publication date:
2016-10

Permanent link:
https://doi.org/10.3929/ethz-b-000116631

Originally published in:
Biomolecular NMR Assignments 10(2), https://doi.org/10.1007/s12104-016-9682-y

Funding acknowledgement:
146757 - NMR studies in the Solid State (SNF)
159707 - NMR studies in the Solid State (SNF)

Solid-state NMR sequential assignment of an Amyloid-β(1-42) fibril polymorph

Francesco Ravotti[a§], Marielle Aulikki Wälti[a§], Peter Güntert[b,c*], Roland Riek[a*], Anja Böckmann[d*] and Beat H. Meier[a*]

§: Both authors contributed equally.

[a]Physical Chemistry, ETH Zürich

Vladimir-Prelog-Weg 2

8093 Zürich (Switzerland)

E-Mail: beme@ethz.ch, roland.riek@phys.chem.ethz.ch

[b]Institute of Biophysical Chemistry, Center for Biomolecular Magnetic Resonance, Goethe University Frankfurt am Main, Max-von-Laue-Str. 9, 60438 Frankfurt am Main, Germany

[c]Department of Chemistry, Graduate School of Science and Engineering, Tokyo Metropolitan University, 1-1 Minami-Ohsawa, Hachioji, Tokyo 192-0397, Japan

E-Mail: guentert@em.uni-frankfurt.de

[d]Institut de Biologie et Chemie des Protéines, Bases Moléculaires et Structurales des Systèmes Infectieux, Labex Ecofect, UMR 5086 CNRS, Université de Lyon

7 passage du Vercors

69007 Lyon (France)

E-Mail: a.bockmann@ibcp.fr

Abstract

The formation of fibrils of the amyloid-β (Aβ) peptide is considered to be a key event in the pathology of Alzheimer's disease (AD). The determination of a high-resolution structure of these fibrils is relevant for the understanding of the molecular basis of AD. In this work, we present the sequential resonance assignment of one of the polymorphs of Aβ(1-42) fibrils. We show that most of the protein is rigid, while a stretch of 4 residues (11-14) is not visible by solid-state NMR spectroscopy due to dynamics.

Keywords

Alzheimer's disease; Amyloid-β peptide; amyloid fibrils; solid-state NMR spectroscopy;

Biological context

AD is a neurodegenerative disorder accompanied by accumulation and aggregation of Aβ leading to extracellular plaques in the brain that, according to the amyloid hypothesis, is considered a key event in the disease (Selkoe et al. 1991, Hardy et al. 2002). Aβ is a peptide of 39–43 amino-acid

residues, which is produced in neurons from the β-amyloid precursor protein (APP) via sequential cleavage by β- and γ-secretases (Masters et al. 1985, Kang et al. 1987). From the various species, Aβ(1-40) and Aβ(1-42) are the most abundant fragments present in human brain and Aβ(1-42) is considered to be more neurotoxic and tends to aggregate faster than Aβ(1-40) (Masters et al. 1985, Ovchinnikova et al. 2011, Selkoe et al. 1994). The characterization of the structure of these Aβ(1-42) fibrils is crucial for a profound understanding of AD, as well as for devising strategies for the development of interacting compounds. Solid-state NMR can deliver atomic-resolution structural models. (Lu et al. 2013; Schütz et al. 2015; Xiao et al. 2015) A major challenge in the study of amyloids is their appearance in a variety of 3D structures, the so-called polymorphs.(Meier and Böckmann 2015). This is, the 3D structure is not only defined by the amino-acid sequence, but also by the conditions used for the fibrillization. Here we characterous a virtually homogeneous sample of Aβ(1-42) fibrils, leading to single set of peaks in the 20 ms DARR spectrum (Fig. 1).

Methods and experiments

Sample preparation of [U-^{13}C,^{15}N] A β (1-42) fibrils

Expression and purification

The production of recombinant Aβ(1-42) has been described previously. (Wälti et al. 2015) Briefly, the expression was performed in *Escherichia coli* (BL21(DE3)) in standard ^{15}N and ^{13}C isotope labeled minimal media. The cells were induced at an OD_{600} ~1.3 at 37 °C for 12 hours. The protein containing a N-terminal hexahistidine tag was purified by a Nickel-NTA agarose column and further by reversed-phase chromatography (RPC). The cleavage was subsequently performed with tobacco etch virus (TEV) protease in order to obtain the correct sequence of Aβ(1-42). Furthermore, the peptide was purified with a second RPC and finally lyophilized. The high purity of the peptide was affirmed by silver-stained SDS-polyacrylamide gels and mass spectrometry.

Fibrillization

The purified Aβ(1-42) peptide was dissolved in 10 mM sodium hydroxide (NaOH) after some minutes of incubation time, a sonication bath was used to increase the soluble fraction (3 times 30 seconds sonication with 50-60% power, interrupted by 1 minute cooling on ice). In order to remove large aggregates the sample was centrifuged for 1 h at 126'000 g at room temperature with an airfuge. If required the sample was further diluted with 10 mM NaOH in order to reach a final concentration of 60 µM peptide. The phosphate buffer including the respective additives was added in order to reach a final concentration of 30 µM Aβ(1-42) in 100 mM H_3PO_4-NaOH pH 7.4, 100 mM NaCl, and 100 µM $ZnCl_2$. The fibrillization was induced with the addition of 10% preformed Aβ(1-42) seeds at 350 revolutions pre minute (rpm) at 37 °C and incubated for 2 weeks. The seeding was done for 3 generations, 10% of the grandparent generation were used as seeds for the parent generation, and again 10% for the daughter generation; whereas the formation of each generation was lasting one week. An elecromicrograph sowing the fibril morphology is shown in Figure 1.

Sample preparation for solid-state NMR measurements

The obtained fibrils with a quantity of 15-20 mg peptide were centrifuged at 30'000 g over night (SW41-TI swinging bucket, optima L90-K, Beckmann) and resuspended in MilliQ water. The fibrils were washed for 3 days by gently shaking. The pellet was again centrifuged at 30'000 g over night, the supernatant was discarded and the fibrils were packed into a 3.2 mm Bruker rotor by ultrazentrifugation using a filling device. (Böckmann et al. 2009) The drive tip was sealed with epoxy glue (Araldit® blue) in order to prevent the dehydration of the fibrils during the experiment.

NMR spectroscopy

Solid-state NMR spectroscopy

All spectra for the sequential assignment were measured on a Bruker Avance II+ 850 MHz with magic-angle spinning (MAS) at 19 kHz

using a Bruker 3.2 mm triple-resonance probe. The sample temperature was determined, using the water resonance frequency, to be around 4 °C. All spectra were apodized with a Shifted Sine Bell window function (SSB of 2.2 – 2.7). The processing was done by PROSA (Güntert et al. 1992) and TopSpin 3.1 (Bruker Biospin) and the analysis was performed with CcpNMR analysis 2.3 (Vranken et al. 2005; Stevens et al. 2011). We performed the standard set of 3D assignment spectra, namely NCOCX, NCACX, NCACB, CCC and CANCO (Schuetz et al. 2010), and in addition 2D DARR, NCO and NCA. All experimental parameters are displayed in Table 1.

Assignment and data deposition

The fibrils of Aβ(1-42) analyzed in this work show in average a linewidth of 0.5 ppm in ^{13}C-^{13}C correlation spectra (Fig. 2a and 2b). A single set of resonances can be identified in the DARR and NCA of Fig. 2 with, a few additional resonances, which were visible in 2D spectra, but not be detected in 3D spectra. We believe that these resonances represent a minor polymorph. The intensity of the intra-residue cross peaks of those resonances is less than 5% of the main form.

NCOCX, NCACX, NCACB, and CANCO spectra allowed the sequential assignment of the backbone atoms of the protein (excluding residues 11-14, which were not visible in any of the spectra). 3D CCC and 2D DARR spectra were recorded to complete the assignment of the side-chains. (Schuetz et al. 2010; Habenstein et al. 2011)

Using these 3D and 2D spectra, we were able to assign 90.5 % of the backbone and 77 % of the side-chains atoms (90.5 % of nitrogen, and 80.5 % of all carbon atoms, respectively) as demonstrated in Fig. 2, which shows the assigned 2D DARR and 2D NCA spectra, respectively. A representative sequential walk using the NCACX, NCOCX, and CANCO spectra is depicted in Fig. 3. Furthermore, the sequential assignment graph reflecting the completeness of the assignments on a residue-per-residue basis is shown in Fig. 4.

The chemical shifts have been deposited in the BMRB under the accession number 26692.

In order to assess whether the resonances for residues 11-14 are missing due to fast dynamics, we performed a ^{1}H–^{15}N INEPT-based 2D correlation experiment to check for the presence of highly flexible residues in the fibrils. However, this spectrum was devoid of any peaks (data not shown). We therefore think that the missing 4-residues stretch presents an intermediate range (μs correlation times) of motion, rendering it “invisible” in CP as well as INEPT-based experiments. A similar behaviour was observed in (Colvin et al. 2015).

From the chemical-shift information, secondary structure elements can be identified, analyzing the differences of the $^{13}C\alpha$ and $^{13}C\beta$ shifts of each amino-acid residue to the shifts found in a random-coil state.(Wishart and Sykes 1994) In this study, the random-coil shifts were taken from Wang et al. 2002. The resulting secondary chemical shifts show that the fibrils studied here are composed of five short β-strands distributed along the sequence: residues 2–6 (β1), 15–18 (β2), 26–28 (β3), 30–32 (β4), 39–42 (β5) (Fig. 5). In this conservative secondary structure determination we define a beta strand by at least three consequtive resonances with a value the secondary shifts difference $\Delta\delta C\alpha$-$\Delta\delta C\beta$ <-1.4 ppm (Wishard and Sykes. 1994). Just requesting that $\Delta\delta C\alpha$-$\Delta\delta C\beta$ is negative would add another beta strand at residues 20-22 (light red in Fig.5).

Figure 6 shows a comparison of chemical shifts of the present study with previously published sequential assignments of both Aβ(1-42) and Aβ(1-40) fibrils. Interestingly, the chemical shifts of the Aβ(1-42) fibrils described by both the Griffin (Colvin et al. 2015) and Ishii (Xiao et al. 2015) groups are largely coincident with the presented assignment for residues 16 to 42, with somewhat larger differences for residues 39 and 42. In contrast, significant differences of up to 4 ppm are found in the N-terminal 10 residues. Furthermore, while in the present study the N-terminal residues (D1-Y10) show peaks in the 20 ms DARR spectrum, they are absent in the study by Colvin et al. These findings indicate that in the various Aβ(1-42) fibrils characterized so far, the core structure of residues 16-42 is similar, while the N-terminal segment comprising residues 1-15

might be structurally distinct.

The influence of Zn^{2+} on fibrillization was investigated by (Mithu et al. 2011). They reported no complete assignments but for the residues characterized the values for all conformers obtained in the presence or absence of Zn^{2+} differ considerably from the ones for the polymorph investigated in this assignment note.

In a comparison of the presented Aβ1-42) assignment with those obtained from different fibril preparations of Aβ(1-40) ((Paravastu et al. 2008; Bertini et al. 2011) including the Aβ(1-40) Osaka mutant (Huber et al. 2015), significant chemical-shift differences are observed throughout the entire amino-acid sequence. These findings indicate that the structures of the fibrils of these polymorphs of Aβ(1-42) and Aβ(1-40) are structurally distinct. We conclude that the three preparations of Aβ(1-42) discussed comprise essentially the same conformatiom for residues 17-42, while the N-terminal residues 1-16 are partially or fully disordered and might be different from preparation to preparation. In contrast, the Aβ(1-42) fibrils are structurally distinct from known Aβ(1-40) fibrils along the entire sequence.

Acknowledgment
This work was supported by grants from Schweizerischer Nationalfonds zur Förderung der Wissenschaftlichen Forschung (200020_146757 and 200020_159707) and the ETH Zürich Research Commission TH 16 09-3 to BHM and by grants ANR-12-BS08-0013-01 and ANR-14-CE09-0024B from the Agence Nationale de la Recherche to AB.

References

Bertini I, Gonnelli L, Luchinat C, et al (2011) A New Structural Model of Aβ40 Fibrils. J Am Chem Soc 133:16013–16022. doi: 10.1021/ja2035859

Böckmann A, Gardiennet C, Verel R, et al (2009) Characterization of different water pools in solid-state NMR protein samples. J Biomol NMR 45:319–327. doi: 10.1007/s10858-009-9374-3

Colvin MT, Silvers R, Frohm B, et al (2015) High Resolution Structural Characterization of Aβ 42Amyloid Fibrils by Magic Angle Spinning NMR. J Am Chem Soc 137:7509–7518. doi: 10.1021/jacs.5b03997

Habenstein B, Wasmer C, Bousset L, et al (2011) Extensive de novo solid-state NMR assignments of the 33 kDa C-terminal domain of the Ure2 prion. J Biomol NMR 51:235–243. doi: 10.1007/s10858-011-9530-4

Huber M, Ovchinnikova OY, Schütz AK, et al (2015) Solid-state NMR sequential assignment of Osaka-mutant amyloid-beta (Aβ1-40 E22Δ) fibrils. Biomol NMR Assign 9:7–14. doi: 10.1007/s12104-013-9535-x

Lu J-X, Qiang W, Yau W-M, et al (2013) Molecular Structure of beta-Amyloid Fibrils in Alzheimer's Disease Brain Tissue. Cell 154:1257–1268. doi: 10.1016/j.cell.2013.08.035

Meier BH, Böckmann A (2015) The structure of fibrils from "misfolded" proteins. Current Opinion in Structural Biology 30:43–49. doi: 10.1016/j.sbi.2014.12.001

Mithu VS, Sarkar B, Bhowmik D, et al (2011) Zn(++) binding disrupts the Asp(23)-Lys(28) salt bridge without altering the hairpin-shaped cross-β Structure of Aβ(42) amyloid aggregates. Biophys J 101:2825–2832. doi: 10.1016/j.bpj.2011.10.023

Paravastu AK, Leapman RD, Yau W-M, Tycko R (2008) Molecular structural basis for polymorphism in Alzheimer's beta-amyloid fibrils. P Natl Acad Sci USA 105:18349–18354. doi: 10.1073/pnas.0806270105

Schuetz A, Wasmer C, Habenstein B, et al (2010) Protocols for the sequential solid-state NMR spectroscopic assignment of a uniformly labeled 25 kDa protein: HET-s(1-227). Chembiochem 11:1543–1551. doi: 10.1002/cbic.201000124

Schütz AK, Vagt T, Huber M, et al (2015) Atomic-Resolution Three-Dimensional Structure of Amyloid β Fibrils Bearing the Osaka Mutation. Angew Chem Int Ed Engl 54:331–335. doi: 10.1002/anie.201408598

Stevens TJ, Fogh RH, Boucher W, et al (2011) A software framework for analysing solid-state MAS NMR data. J Biomol NMR 51:437–447. doi: 10.1007/s10858-011-9569-2

Vranken WF, Boucher W, Stevens TJ, et al (2005) The CCPN data model for NMR spectroscopy: development of a software pipeline. Proteins 59:687–696. doi: 10.1002/prot.20449

Wälti MA, Orts J, Vögeli B, et al (2015) Solution NMR studies of recombinant Aβ(1-42): from the presence of a micellar entity to residual β-sheet structure in the soluble species. Chembiochem 16:659–669. doi: 10.1002/cbic.201402595

Wishart DS, Sykes BD (1994) The 13C Chemical-Shift Index: A simple method for the identification of protein secondary structure using 13C chemical-shift data. J Biomol NMR 4:171–180. doi: 10.1007/BF00175245

Xiao Y, Ma B, McElheny D, et al (2015) Abeta;(1-42) fibril structure illuminates self-recognition and replication of amyloid in Alzheimer's disease. Nat Struct Mol Biol 22:1–9. doi: 10.1038/nsmb.2991

Tables and Figures

Table 1: Experimental parameters used for the solid-state NMR experiments for the assignment of the Aβ(1-42) peptide resonances in the fibrils.

Experiment	**NCACX**	**NCOCX**	**NCACB**	**CANCO**	**CCC**	**NCA**	**NCO**	**DARR 20ms**
MAS frequency [kHz]	19	19	19	19	19	19	19	19
Transfer 1	HN-CP	HN-CP	HN-CP	HC-CP	HC-CP	HN-CP	HN-CP	HC-CP
field [dB] -^{1}H	3	3	3	2	3	3	3	3
field [kHz] -^{1}H	80.3	80.3	80.3	90.1	80.3	80.3	80.3	74.9
field [dB] -X	-2	-2	-2	-1.5	-1.3	-2	-2	0.1
field [kHz] -X	57.4	57.4	*57.4*	*70.2*	*67.8*	*57.4*	57.4	*57.6*
shape	tangent	tangent	tangent	tangent	tangent	tangent	tangent	tangent
carrier [ppm]	-	-	-	CA	-	-	-	-
time [ms]	1.4	1.4	1.4	0.38	0.35	1.4	1.4	0.9
Transfer 2	NC-CP	NC-CP	NC-CP	CN-CP	DREAM	NC-CP	NC-CP	DARR
field [dB] -^{1}H	-	-	-	-	2	-	-	15
field [kHz] -^{1}H	-	-	-	-	90.1	-	-	18.7
field [dB] -^{13}C	21	21	21	21	16	21	21	-
field [kHz] -^{13}C	5.2	5.2	5.2	5.2	9.2	5.2	5.2	-
field [dB] - ^{15}N	6.1	6.2	6.1	6	-	6.1	6.2	-
field [kHz] - ^{15}N	22.5	22.3	22.5	22.8	-	22.5	22.3	-
shape	tangent	tangent	tangent	tangent	tangent	tangent	tangent	-
carrier [ppm]	CA	CO	CA	CA	52	CA	CO	-
time [ms]	7	7	7	7	4	7	7	20
Transfer 3	DARR	DARR	DREAM	NC-CP	DARR	-	-	-
field [dB] -^{1}H	15	15	2.1	-	15	-	-	-
field [kHz] -^{1}H	20.1	20.1	89.1	-	20.1	-	-	-
field [dB] -^{13}C	-	-	16.2	21	-	-	-	-
field [kHz] -^{13}C	-	-	9.1	5.2	-	-	-	-
field [dB] - ^{15}N	-	-	-	6.2	-	-	-	-
field [kHz] - ^{15}N	-	-	-	22.3	-	-	-	-
shape	-	-	tangent	tangent	-	-	-	-
carrier [ppm]	-	-	52	CO	-	-	-	-
time [ms]	80	65	4	7	80	-	-	-
t_1 increments	96	112	100	92	200	768	768	2560
sweep width (t_1) [kHz]	6	7	7	8	20	40	40	100
max. acq time (t_1) [ms]	8.00	8.00	7.14	5.75	5.00	9.60	9.60	12.80
t_2 increments	100	76	108	108	200	1536	1536	3968
sweep width (t_2) [kHz]	8	6	9	7	20	50	50	100
max. acq time (t_2) [ms]	6.25	6.33	6.00	7.71	5.00	15.36	15.36	19.84
t_3 increments	2560	2560	2048	2560	2560	-	-	-
sweep width (t_3) [kHz]	100	100	100	100	100	-	-	-
max. acq time (t_3) [ms]	12.8	12.8	10.24	12.8	12.8	-	-	-
^{1}H Spinal64 Decoupling power [kHz]	90	90	90	90	90	90	90	90

interscan delay [s]	2.5	2.5	2	2.9	2.1	2.5	2.5	3
number of scans	8	8	8	8	4	16	16	8
total measurement time [h]	53.7	47.6	48.4	64.3	93.7	8.6	8.6	17.3

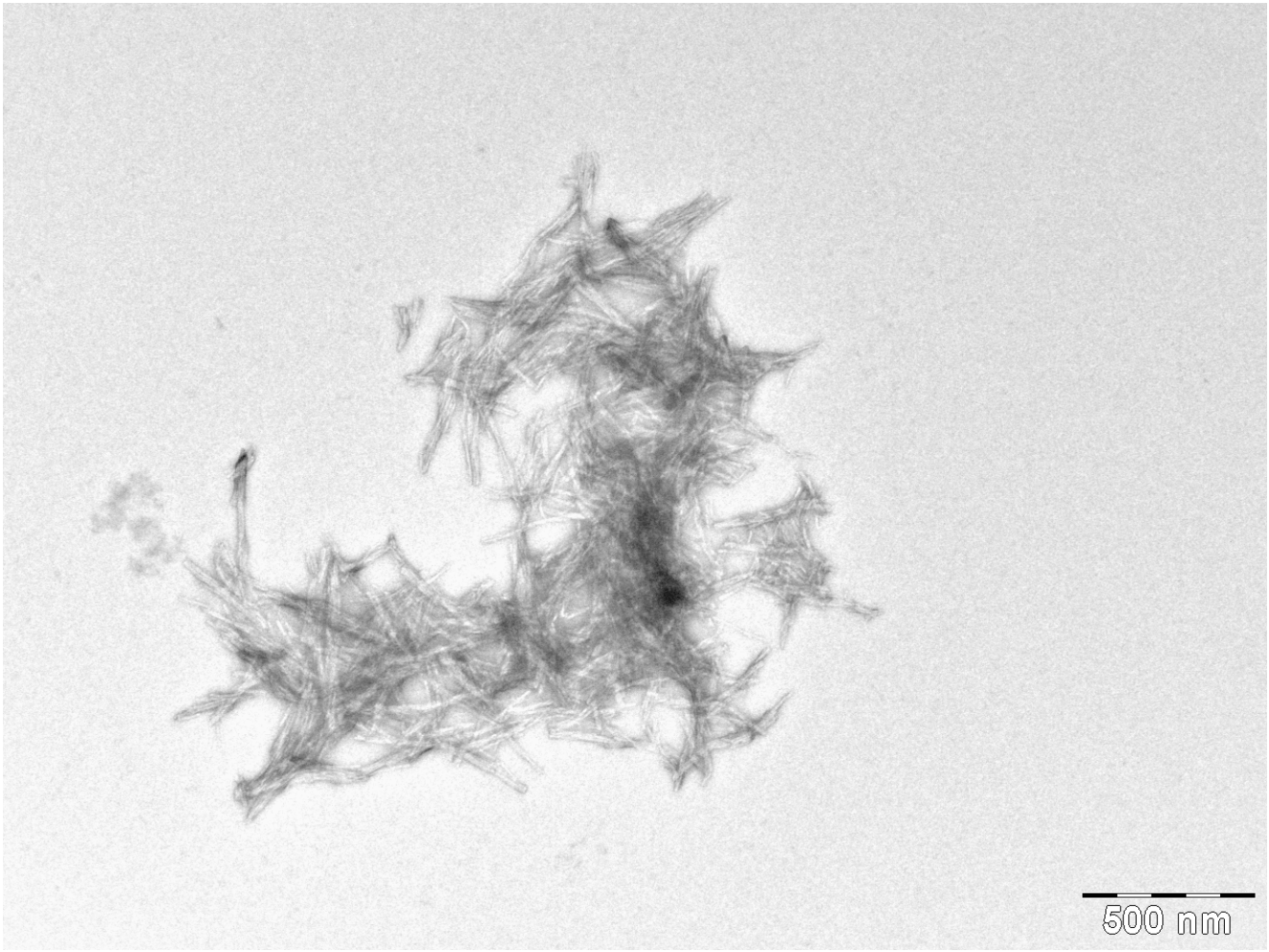

Fig. 1 Transmissionelectromicrograph of the negatively stained fibrils of the form used in this study.

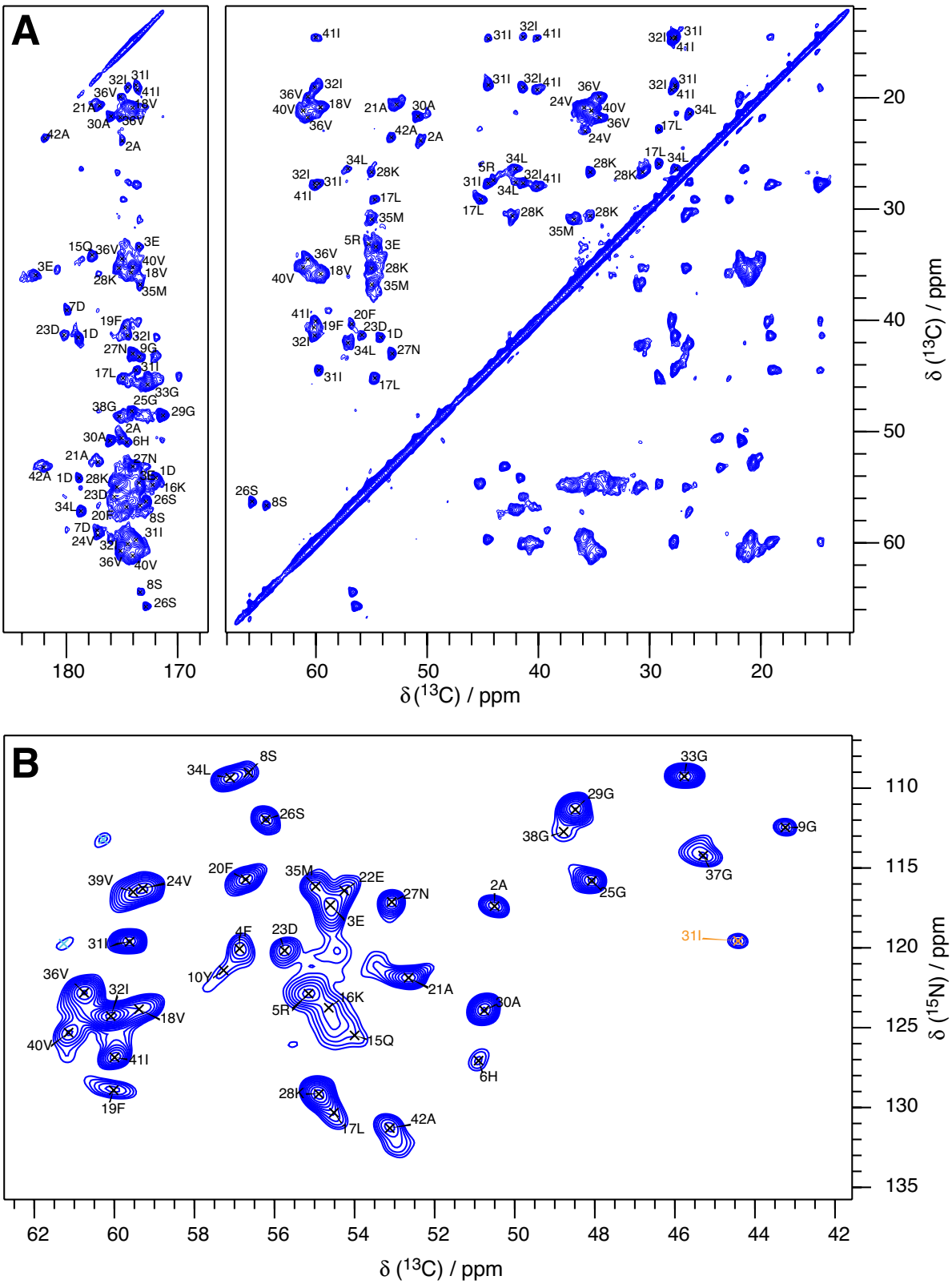

Fig. 2 2D solid-state NMR spectra of uniformly ^{13}C,^{15}N-labeled Aβ(1-42) fibrils measured at a magnetic field of 20.0 T and 17 kHz MAS. A) 2D ^{13}C – ^{13}C DARR spectrum with a mixing time of 20 ms. B) 2D NCA spectrum.The signal with the red label corresponds to a N-Cβ relayed peak, the two weak signals with cyan croses to a minor polymorph.

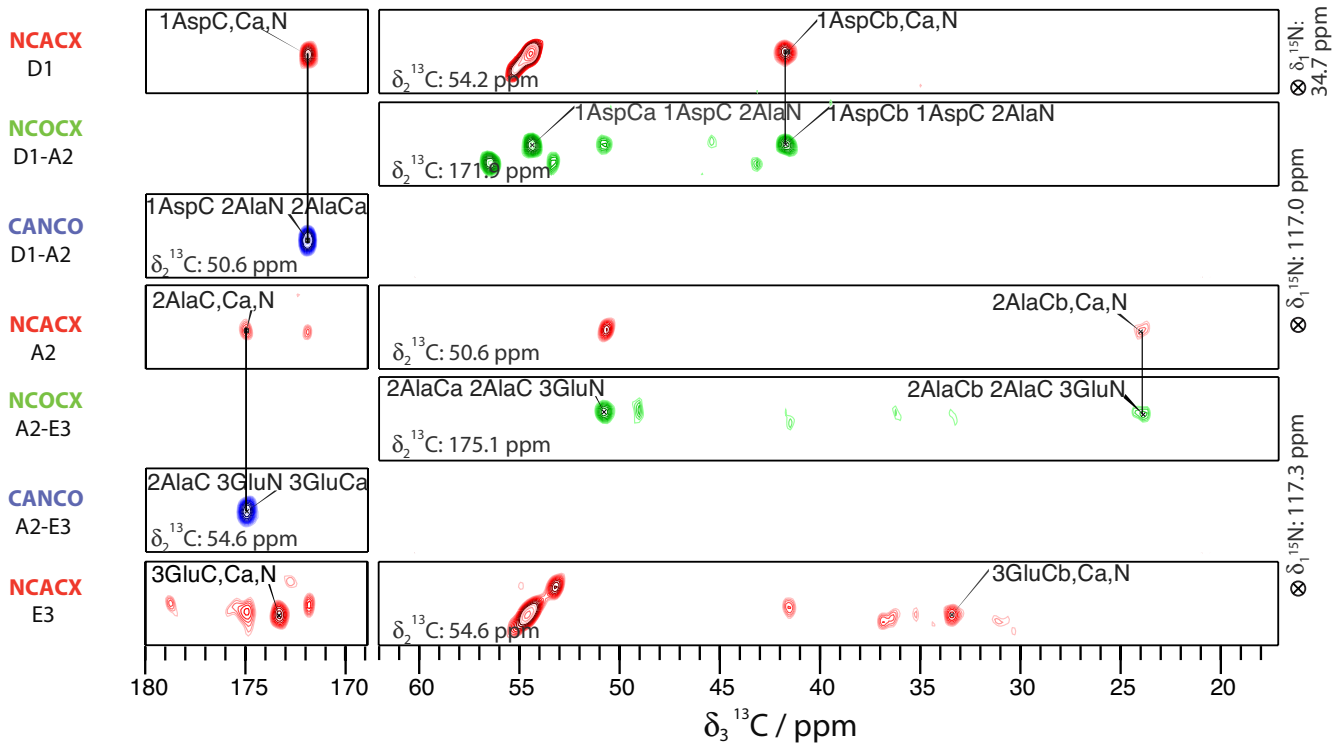

Fig. 3 3D solid-state NMR spectra of Aβ(1-42) fibrils (19 kHz MAS, 20 T B_0) for the sequential assignment. Extracts of NCACX (red), CANCO (blue), and NCOCX (green) spectra are shown, demonstrating a sequential walk starting from the N-terminus. The connection of residues D1 to A2 and further to E3 are illustrated by vertical lines.

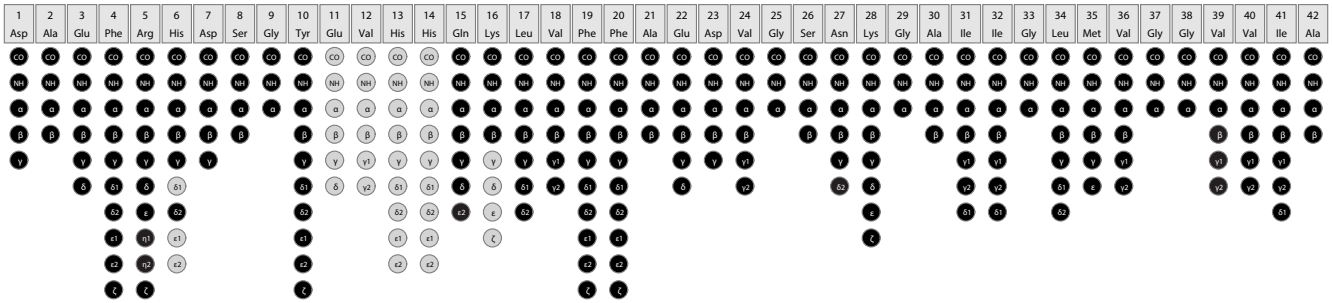

Fig. 4 Sequential assignment graph showing all carbon and nitrogen atoms of Aβ(1-42) by circles. The assigned atoms are shown in black, whereas the unassigned ones are shown in grey. The graph was designed with the software CcpNMR 2.3 (Stevens et al. 2011, Vranken et al. 2005)

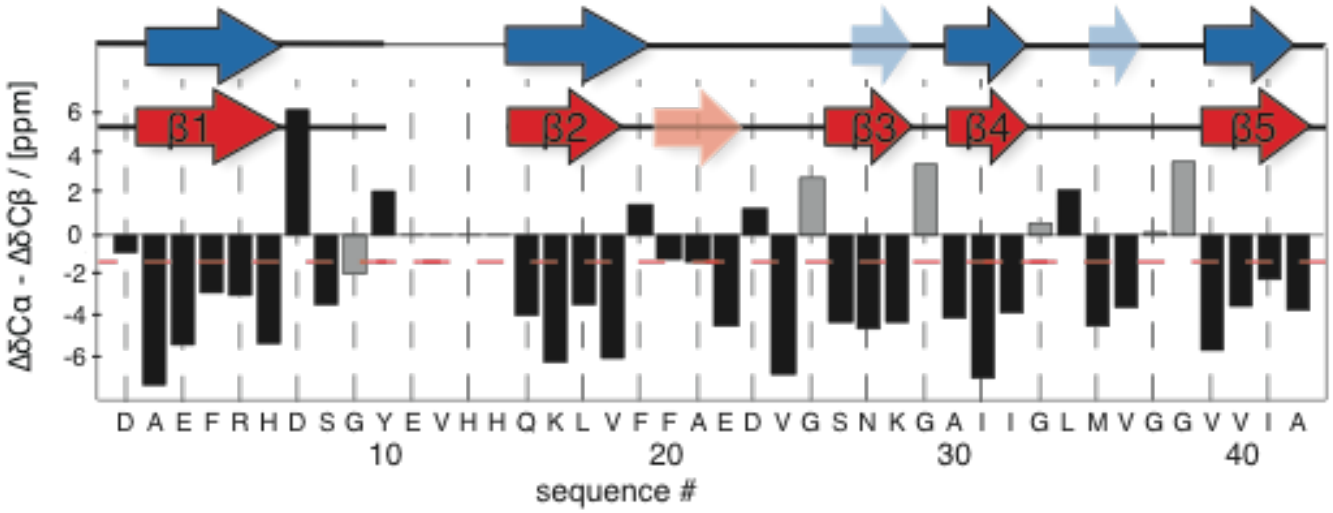

Fig. 5 Top: Secondary structural elements in red as predicted from secondary shifts (see below) and in blue as prediced by TALOS+. The line is interrupted where data are missing. Bottom: C^{α} and C^{β} chemical shift differences in respect to the corresponding random coil values are displayed below. Red β-strands are assumed where the secondary chemical shifts (Wishard and Sykes 1994) are lower than -1.4 ppm for three residues in a row. Blue β-strands are assumed when TALOS predics β-conformation for at least three residues in a row. In addition possible light blue strands are marked in light blue of two residues ina row are predicted beta-strand by TALOSAn additional putative beta strand with three negative values in a row but not reaching the -1.4 ppm limit is indicated in light red. For the glycines, the $\Delta\delta C^{\alpha}$ shifts are displayed in grey.

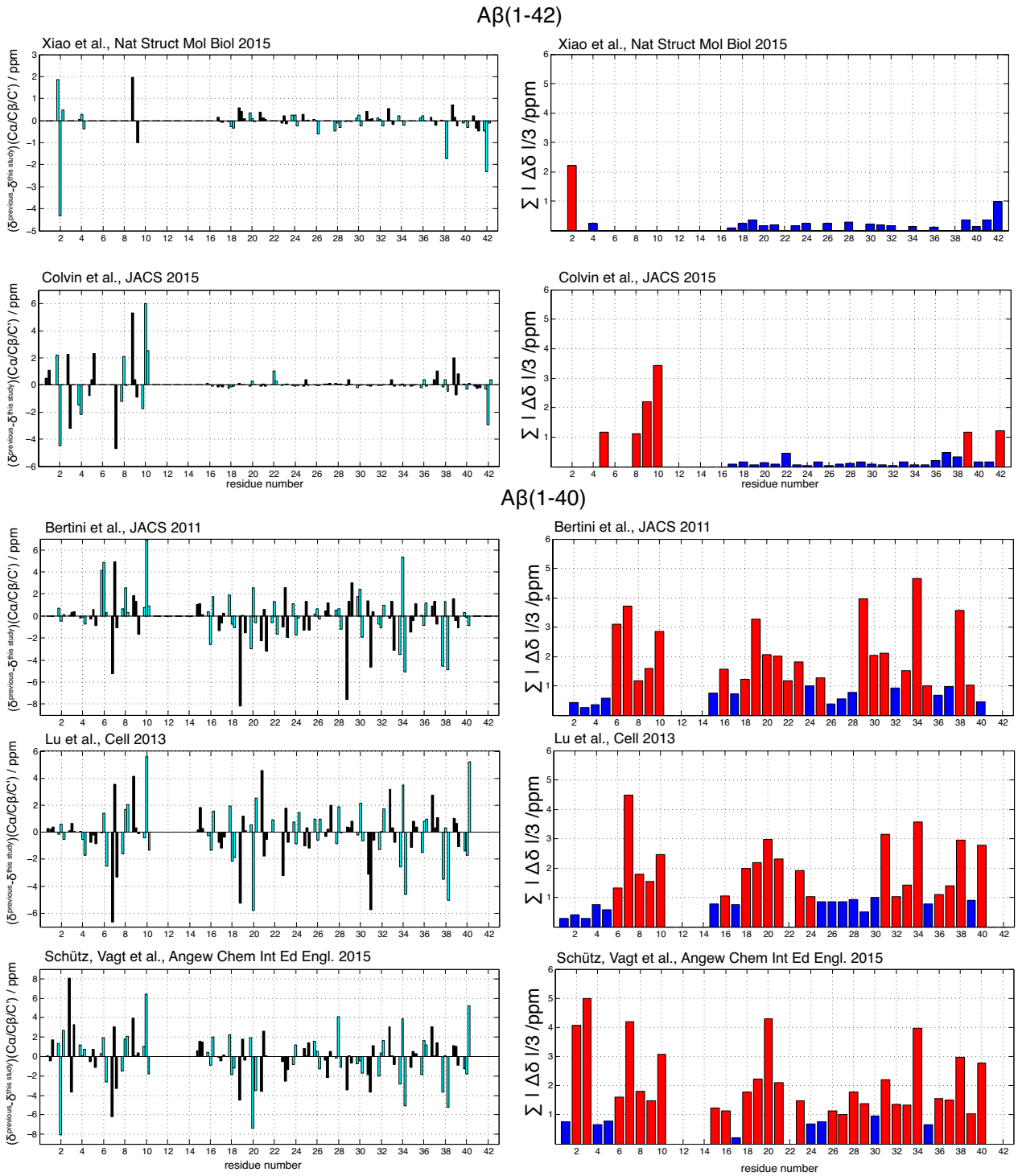

Fig. 6 Left: differences between chemical shifts of the Aβ(1-42) fibrils of this study with previously published Aβ fibrils (Aβ(1-42) fibrils (Xiao et al. 2015, Colvin et al. 2015), Aβ(1-40) fibrils (Bertini et al. 2011, Paravastu et al. 2008) and Aβ(1-40) E22Δ fibrils (Schütz, Vagt et al. 2015). The first bar of each residue shows the chemical shift difference of ^{13}Cα, the second ^{13}Cβ, and the third ^{13}C', respectively. For readability of the graphs the bars of the even residues are color coded in cyan and the odd ones in black, respectively. Right: residue-resolved average absolute values of the ^{13}Cα, ^{13}Cβ, and ^{13}C' chemical shift differences between chemical shifts of the Aβ(1-42) fibrils of this study with previously published Aβ fibrils with $\sum|\Delta\delta|/3=(|\delta C\alpha^{previous} - \delta C\alpha^{this\ study}| + |\delta C\beta^{previous} - \delta C\beta^{this\ study}| + |\delta C'^{previous} - \delta C'^{this\ study}|)/3$. Bars with differences larger than 1 ppm are depicted in red, the ones equal or smaller in blue.